Impact of a human gut microbe on *Vibrio cholerae* host colonization through biofilm enhancement

Kelsey Barrasso[1,2], Denise Chac[3], Meti D. Debela[4], Jason B. Harris[4,5], Regina C. LaRocque[4], Firas S. Midani[6], Firdausi Qadri[7], Jing Yan[8], Ana A. Weil[3,*], Wai-Leung Ng[1,2,*]

Affiliations:

1. Department of Molecular Biology and Microbiology, Tufts University School of Medicine, Boston, MA
2. Program of Molecular Microbiology, Graduate School of Biomedical Sciences, Tufts University School of Medicine, Boston, MA
3. Department of Medicine, University of Washington, Seattle, WA
4. Division of Infectious Diseases, Massachusetts General Hospital, Boston, MA
5. Department of Pediatrics, Harvard Medical School, Boston, MA
6. Department of Molecular Virology and Microbiology at Baylor College of Medicine, Houston, TX
7. International Center for Diarrheal Disease Research, Bangladesh, Dhaka, Bangladesh
8. Department of Molecular, Cellular and Developmental Biology, Yale University, New Haven, CT

* Co-corresponding authors/equal contributions

Corresponding authors: Ana A. Weil and Wai-Leung Ng

Email: anaweil@uw.edu wai-leung.ng@tufts.edu

Author Contributions:

- Designed research (KB, DC, JY, AAW, WLN)
- Performed research (KB, DC, MDD, JY)
- Contributed new reagents or analytic tools (FSM, JY, JBH, RCL, FQ)
- Analyzed data (KB, DC, FSM, JY, AAW, WLN)

- Wrote the paper (KB, DC, JY, AAW, WLN)

Competing Interest Statement: No competing interests.

Classification: Biological Sciences- Microbiology

Keywords: Bacterial pathogenesis, gut microbiome, mixed species biofilm

This PDF file includes:

Main Text
Figures 1 to 8

Abstract

The human intestinal microbiota plays a crucial role in protection against the infection of *Vibrio cholerae,* the etiological agent of the diarrheal disease cholera. A rare commensal bacterium, *Paracoccus aminovorans,* was previously identified to bloom in the intestines during *V. cholerae* infection in a cohort of patients exposed to the pathogen. However, how *P. aminovorans* interacts with *V. cholerae* has not been experimentally determined; moreover, whether any association between this bacterium alters the behaviors of *V. cholerae* to affect the disease outcome is also unclear. Here we show that *P. aminovorans* and *V. cholerae* together form dual-species biofilm structures with previously uncharacterized novel features. Using an infant mouse colonization model, we demonstrate that the presence of *P. aminovorans* within the murine small intestine enhances *V. cholerae* colonization in the same niche that is dependent on the production of the *Vibrio* exopolysaccharide (VPS), a major component of mature *V. cholerae* biofilm. Our study has identified a novel mechanism by which a microbiota species increases *V. cholerae* virulence, and we establish a plausible explanation for the increased abundance of specific microbiota species in individuals during *V. cholerae* infection.

Significance Statement

While ample evidence suggests that the outcome of various enteric infections can be affected by the intestinal microbiota, how specific gut microbes change the behaviors of a pathogen is unclear. Here we characterize the interaction between *Vibrio cholerae* and a rare gut microbe, *Paracoccus aminovorans*, that is known to bloom in the intestines during active *V. cholerae* infection. These two bacteria form a dual-species biofilm structure and increases the host colonization efficiency of *V. cholerae*. To our knowledge, no prior study has demonstrated that an individual microbe increases *V. cholerae* virulence. Importantly, our study illustrates a novel mechanism of gut microbe-pathogen interaction that has the potential to alter the disease outcome.

Main Text

Introduction

Vibrio cholerae (*Vc*) causes an estimated 3 million infections and 120,000 deaths each year, and larger and more deadly outbreaks have increased during the last decade (1, 2). A wide range of clinical outcomes occur in persons exposed to *Vc*, ranging from asymptomatic infection to severe secretory diarrhea. It is nearly certain that many behaviors of *Vc* in the aquatic environment and

inside the host are significantly affected by the presence of other microbes (3), and recent studies have provided strong evidence that the gut microbiota may impact severity of cholera (4-7). Several functions of the gut microbiota influence the growth or colonization of enteric pathogens, including production of anti-microbial compounds, maintenance of the intestinal barrier, regulation of the host immune response, and modulation of available nutrients (8). Gut microbes have been shown to have an important role in *Vc* infection in various animal models. For instance, disruption of the commensal microbiota with antibiotics is required to allow successful *Vc* colonization of adult rodent animals (9, 10). Conversely, *Vc* actively employs a Type VI secretion system to attack host commensal microbiota to enhance colonization of the gut in infant mice (11). Moreover, specific microbial species have profound impact on *Vc* colonization. *Blautia obeum*, an anaerobic Gram-positive bacterium, decreases *Vc* intestinal colonization by producing a signaling molecule that induces *Vc* into a high cell-density quorum sensing state (5) in which virulence gene expression is repressed (12, 13). Certain microbiota species reduce *Vc* colonization by producing an enzyme called bile salt hydrolase that degrades and lowers the amount of the host-produced virulence-activating compound taurocholate (4, 5). Through metabolizing host glycans into short chain fatty acids that suppresses *Vc* growth, a prominent commensal species, *Bacteroides vulgatus,* reduces *Vc* proliferation within the intestine (14).

While the above studies exemplify how a single microbe or a group of microbes can protect the host from *Vc* infection, the mechanism used by certain gut microbes to promote *Vc* virulence, thereby increasing the susceptibility of individuals to contract cholera and worsen disease outcomes, is less well understood. We have previously studied household contacts of cholera patients to understand gut microbes that impact susceptibility to cholera and identified gut microbes associated with increased or decreased susceptibility to *Vc* infection (6, 7). We also observed that the gut microbial species *Paracoccus aminovorans* (*Pa*) was statistically more abundant in the gut microbiota during *V. cholerae* infection (7). To determine the underlying mechanisms behind these correlative clinical findings, we evaluated the relationship between *Pa* and *Vc* in co-culture and determined the effects of *Pa* on *Vc* infection outcomes with *in vivo* models. Here we show that *Pa* interacts directly with *Vc* to form dual-species biofilm structures with previously uncharacterized features. Moreover, *Vc* colonization inside the animal host is enhanced by pre-colonization of *Pa* in the small intestine that is dependent upon *Vc* biofilm production. Our findings suggest a novel mechanism used by a gut microbe to specifically associate with *Vc* and indicate that the increased abundance of *Pa* in the infected individuals is unlikely to be coincidental. The unusual association between these two species may have a direct impact on *Vc* pathogenesis and alter the outcome of *Vc* infection in humans.

Results

P. aminovorans is significantly more abundant in individuals with active *V. cholerae* infection.

Paracoccus is a genus of soil microbes also found in the gut microbiome of humans (15, 16). Our previously published analysis of stool gut microbes from household contacts of cholera patients described that *P. aminovorans (Pa*) was found to be present during active *V. cholerae* infection in some study participants, and was rare in uninfected participants (7). We identified *Pa* as differentially associated with active *V. cholerae* infection (7). *Pa* OTUs in infected compared to uninfected persons were significantly higher as a proportion of the total sequencing reads in the stool of infected participants; six out of 22, or 27% of infected patients, had detectable *Pa* compared to only 5.6% (2/36) of uninfected individuals (Fig. 1). This finding was particularly interesting to us because typically active *V. cholerae* infection results in a drastic reduction of most gut microbes due to diarrhea, vomiting, oral rehydration solution ingestion, antibiotic use, and *V. cholerae* infection itself (17). Although few people were found to harbor *Pa* overall, we found a much higher proportion of *Pa* during infection, and we hypothesized that this organism may be resistant to displacement from the gut during infection. While our previous study demonstrates a positive

correlation between *Pa* in human stool and *V. cholerae* infection, a causal relationship between this gut microbiota species and *V. cholerae* infection had not been previously established.

_Pa_ increases _Vc_ host colonization

We modified a well-established infant mouse colonization model (18) to assess whether pre-colonization with *Pa* in the small intestine would promote *Vc* host colonization. First, we isolated a spontaneous streptomycin resistant ($Strep^R$) mutant derived from the ATCC type strain of *Pa* for selection and enumeration of *Pa* following host colonization. Infant mice (3-day old) were intragastrically inoculated with *Pa* (10^7 colony forming units [CFUs]) every 12 hours for 4 doses (0, 12, 24, 36 hours). At 24 and 48 hours after inoculation, small intestines from these animals were dissected and homogenized. Gut homogenates were serially diluted and plated on medium containing streptomycin to assess *Pa* colonization. $Strep^R$ *Pa* colonies (>10^6 CFUs/intestine) were recovered at these two time points (Fig. 2A), while no $Strep^R$ colony was detected in the mock treated group, indicating *Pa* successfully and stably colonized the small intestines of these animals with this inoculation protocol. Unlike previous studies (9, 10), pretreatment with antibiotics did not change the outcome of *Pa* colonization. However, we found that the use of relatively young animals is critical for establishing *Pa* colonization, and we hypothesize that this is needed because the mature microbiota has not yet established in the infant mouse gut.

We then evaluated if pre-colonization by *Pa* would influence *Vc* colonization in the small intestine. *Pa* pre-colonization in the infant mice was established over a 36-hour period as described above. Negative control animals were inoculated with sterile media in place of *Pa* over the same dosing schedule. Twelve hours after the last *Pa* inoculation (i.e., 48 hours after the first *Pa* inoculation), these animals were infected with *Vc* (10^6 CFU) to evaluate whether pre-colonization with *Pa* had an impact on *Vc* colonization. Compared to the control group, there was a significant increase (10-fold, $p<0.001$) of the *Vc* colonized in the mice pre-colonized with *Pa* (Fig. 2B). To our knowledge, no prior study has demonstrated that individual microbiota species increase *Vc* host colonization. Our results also demonstrate that our microbiome studies in humans (6, 7) can be used a predictive tool to identify gut microbes that alter *Vc* virulence.

_Pa_ promotes biofilm formation of _Vc_

We previously examined the growth of *Vc* in the cell-free spent culture media of different gut microbes, and found that growth was increased in the spent medium harvested from *Pa* compared to that harvested from *Vc* itself (7). To further investigate this observation and determine if there are direct interactions between these two species, *Vc* and *Pa* were co-cultured and incubated at room temperature for three days where both planktonic and biofilm growth of these two species was monitored. Although we do not fully understand the dynamics between *Vc* and *Pa* during natural human infection, the starting ratio between *Vc* to *Pa* was adjusted to 1:10 to mimic the probable ratio at the initiation of infection used in the animal model described above. There was no significant increase in growth in the planktonic phase of either *Vc* or *Pa* in the co-cultures when compared to the cultures containing a single species (Fig. 3A). However, the *Vc*/*Pa* co-culture formed a pellicle at the air-liquid interface that is visibly thicker than that formed by *Vc* mono-culture (Fig. 3B). The *Pa* mono-culture did not form a visible pellicle (not shown). The co-culture pellicle samples were carefully lifted and removed from the culture medium, washed, and broken up to release single cells for enumeration of the number of each species. Compared to *Vc* mono-culture, the co-culture samples contained over 50-fold more *Vc* cells while the ratio of *Vc* to *Pa* increased to approximately 1:1 (Fig. 3C). Recovery of *Pa* in the pellicle was not due to any carryover from the planktonic phase since the medium used for washing the pellicle contained fewer *Vc* and *Pa* cells and quantities of each species were comparable to monoculture controls (Fig. 3D). Therefore, we found that *Vc* and *Pa* coexist stably in the same pellicle structure and the abundance of both *Vc* and *Pa* at the air-liquid interface is promoted by formation of the dual-species pellicle.

Next, we used a standard crystal violet (CV) microtiter plate assay (19) to further evaluate how *Vc* and *Pa* interact under biofilm-inducing conditions. *Vc* and *Pa* were simultaneously inoculated into the wells of microplates with a hydrophilic surface in two different *Vc*:*Pa* ratios (1:1 and 1:10) and

allowed for biofilm formation to occur for 24 hours at 37°C. We also tested if the viability of *Pa* was crucial for this interaction by using heat-killed *Pa* as a control. Consistent with our pellicle composition analysis, *Vc* formed a more robust biofilm than *Pa* under these conditions as demonstrated by increased CV staining in wells containing *Vc* only compared to wells containing *Pa* only (Fig. 4A). Importantly, CV staining was increased in wells containing *Vc* and live *Pa* than in wells with *Vc* only, in a concentration-dependent manner (Fig. 4A). In contrast, CV staining was not significantly higher in wells containing both *Vc* and heat-killed *Pa* than wells with *Vc* only (Fig. 4A). Together, our results suggest that the presence of viable *Pa* significantly increases *Vc* biofilm formation.

To understand what biofilm component is required for *Vc* to interact with *Pa* under these biofilm-inducing conditions, we repeated the above experiments with a *vpsL*$^-$ *Vc* mutant that cannot produce the *Vibrio* exopolysaccharide (VPS) necessary for mature biofilm formation (20). In contrast to what we observed with a *vpsL*$^+$ strain, there was no significant increase in CV staining in wells with both *vpsL*$^-$ mutants and *Pa*, when compared to wells with the *vpsL*$^-$ mutants only (Fig. 4B). These results suggest that the ability of *Vc* to interact with *Pa* under these conditions requires VPS production.

We then tested if the order in which these two species encounter one another is critical for the *Vc* biofilm enhancement phenotype. In humans, *Pa* could either enter the host together with *Vc*, which was modeled using the above biofilm assays; or, *Pa* could be present within the intestinal tract prior to *Vc* infection, since it is a known member of the gut microbiota in humans (7, 15) (Fig. 1), and we modeled this instance in our mouse experiments (Fig. 2). To mimic *Pa* pre-colonization, *Pa* was grown in wells 24 hours before the addition of *Vc*. Similar to our previous results in the co-inoculation experiment, an increase in CV staining was observed in wells where these two species were added sequentially, but not in the wells with *Vc* only (Suppl Fig. 1). Moreover, wells pre-incubated with heat-killed *Pa* and subsequently inoculated with *Vc* had no increase in CV staining compared to wells inoculated with *Vc* alone **(**Suppl Fig. 1). Together, our biofilm quantification data suggest that the presence of *Pa*, regardless of the order of encounter, results in an enhanced biofilm formation of *Vc.*

Structure of *Vc*/*Pa* dual-species biofilm

Based on our analyses described above, we hypothesize that *Vc* and *Pa* form dual-species biofilms. This is unexpected because *Vc* is known to form a clonal community in both *in vitro* and *in vivo* biofilms that are known to exclude other species and even planktonic *Vc* cells (21, 22). Because the pellicle and the CV staining assays are primarily useful for studying biofilms formed at an air-liquid interface (19), we next used high-resolution confocal microscopy (23, 24) to test our dual-species biofilm hypothesis further and to investigate the biofilm structure formed on a solid substratum. With this method, we imaged the three-dimensional (3D) structure of submerged, surface-attached biofilms formed by *Vc* alone and by *Vc*:*Pa* in co-culture (ratio 1:10). All cells in the biofilm were stained with FM 4-64 membrane dye, and *Vc* cells were differentiated from *Pa* using a constitutively produced mNeonGreen reporter (25) expressed from a neutral *Vc* locus (26). At room temperature, a condition known to enhance the formation of *vps*-dependent *Vc* biofilms (27), we observed the characteristic *Vc* biofilm clusters, which remained largely unchanged upon coculturing with *Pa* (Fig. 5 A,B). Similar to our observations in the previous assays, the total biofilm mass quantified from the confocal images increased in the *Vc/Pa* co-culture (Suppl Fig. 2). Upon closer inspection (Fig. 5C), we observed that *Pa* cells occupied the surface areas not colonized by *Vc* and therefore contribute to the increased total biomass. Beyond the surface layer, however, *Pa* cells were largely excluded from the *Vc* biofilm clusters consistent with the clonal nature of *Vc* biofilm (Fig. 5C,D). In *Pa*/*Vc vpsL*$^-$ co-culture (Suppl Fig. 3), our observations of the primary biofilm structure at the surface were unchanged, but three-dimensional clusters above the surface were

not present given the inability of a *vpsL*⁻ mutant to produce the exopolysaccharide required to form mature biofilms.

We also repeated the imaging for co-culture biofilm grown statically at 37°C, a condition under which *Vc* is known to form minimal submerged biofilm (27). Surprisingly, under these conditions *Pa* cells formed a plate-shaped architecture (Fig. 6) that was not present in the *Pa* only culture. Based on this finding, we hypothesize that an unknown substance from *Vc* generates a substratum on which *Pa* cells attach and grow, because *Pa* does not generate these separate structures in the absence of *Vc*. Interestingly, *Vc* cells attached minimally to this substratum as indicated by the sparse mNeonGreen signal in the plate-shape architecture (Fig. 6). The same plate structures were observed in co-culture of *vpsL*⁻ and *Pa* (Suppl Fig. 4), which suggests that this substratum is at least partially made of non-VPS substance. While the exact characteristics of this substratum are unclear, this substance could be stained with FM 4-64, suggesting it contains hydrophobic moieties such as phospholipids (Suppl Fig. 5). Through this series of high-resolution microscopic analyses, we demonstrate that *Vc* and *Pa* can directly and indirectly interact and stably coexist to form a variety of previously uncharacterized 3D biofilm structures under different culture conditions.

Hydrophobic interaction drives *Vc* association with *Pa*

We next turned our attention to investigating what specific features may contribute to the 3D structures formed in the *Pa*/*Vc* dual-species biofilms. As previously reported (7), cell-free spent culture medium collected from *Pa* mono-culture or *Pa*/*Vc* co-culture did not induce *Vc* to form increased biofilm, thus, we excluded the possibility that secreted molecules produced by *Pa* are mediating *Pa/Vc* interaction. We and others have previously shown that *Vc* biofilms are hydrophobic as shown by their high contact angle with water (~110°) (28, 29). Therefore, we hypothesized that hydrophobic interactions may play an important role in the *Pa/Vc* biofilm association (30). To test if *Pa* cells possess surface hydrophobicity that could contribute to their association into *Vc* biofilms, we conducted a standard microbial adhesin to hydrocarbon (MATH) assay (31). We found that the addition of 1ml xylene to 4 ml of *Pa* culture resulted in binding of over 60% of the *Pa* cells to the hydrocarbon, indicating that the *Pa* cell surface is strongly hydrophobic (Fig. 7A). Consistent with this finding, we repeated CV assays using untreated hydrophobic plastic plates, and we found significant CV staining in wells containing *Pa* only, which suggests strong surface adhesion of *Pa* cells (Fig. 7B). The hydrophobicity of *Pa* cells is consistent with their tendency to associate with *Vc* pellicles and to the plate-like *Vc* secretions observed in the submerged biofilms from 37°C incubation experiments. We therefore conclude that the hydrophobic interaction between *Pa* and *Vc* may contribute to the observed physical association *in vitro*. We next evaluated if this interaction contributes to *Vc* infectivity *in vivo.*

Enhancement of *Vc* host colonization by *Pa* depends on biofilm exopolysaccharide production

Biofilm-grown *Vc* cells are known to be more infectious in humans due to increased resistance to gastric pH and increased expression of virulence factors (e.g., such as toxin co-regulated pilus, which mediates host colonization) compared to planktonically grown cells (32-34). We hypothesize that in the presence of *Pa*, *Vc* biofilm formation is enhanced, resulting in increased virulence in the host. In the *in vitro* biofilm assays performed above, we showed that VPS is critical for the interaction between *Pa* and *Vc* under conditions conducive to biofilm formation. To test our hypothesis and measure if the effect of the *Pa/Vc* biofilm interaction impacts host colonization, we compared the colonization efficiency between wild-type (WT) or the *vpsL*⁻ mutants in infant mice with and without *Pa* pre-colonization. As shown previously (35), the *vpsL*⁻ mutant was able to colonize the small intestine equally well as the WT *vpsL*⁺ strain, confirming that the VPS is not absolutely required for host colonization when *Vc* was administrated to the animals alone. In contrast, while *Pa* increased WT *vpsL*⁺ *Vc* colonization, the *vpsL*⁻ mutant did not exhibit the enhanced colonization phenotype in the *Pa* pre-colonized mice (Fig. 8). Together, these findings

suggest that the ability of *Vc* to form a VPS-dependent biofilm is critical for the *Pa*-mediated enhancement of *Vc* colonization.

Discussion

The composition of the gut microbiota can impact the clinical outcomes of enteric infections in humans (36, 37). Several studies have identified commensal species and underlying colonization resistance mechanisms that could be protective against *V. cholerae*. While these studies suggest that microbiota species reduce *Vc* virulence through various mechanisms during the early stages of infection (4, 5, 14), the precise role of these colonization resistance mechanisms in impacting susceptibility to cholera in humans is not known. Interestingly, our previous microbiome study identified specific microbes correlated with differences in *V. cholerae* susceptibility (6, 7), and one of these species, in the genus *Blautia,* correlated with decreased susceptibility to *V. cholerae* infection. A bacterium in this genus was recently found to encode functions that confer colonization resistance (e.g., bile salt hydrolase) to *Vc* infection (4).
While previous studies have identified microbiota-associated mechanisms that are protective against *Vc* infection, to our knowledge, there is not a previous example that identifies an interaction between *Vc* and a human-associated microbiota species that increases *Vc* pathogenicity. We show here that *Pa* pre-colonization promotes *Vc* host colonization, which is consistent with our prior human study in which the presence of *Pa* was differentially abundant in persons infected with *V. cholerae*. This raises the possibility that uncharacterized interactions between *Vc* and other members of the gut microbiota may exacerbate *Vc* virulence and contribute to increased morbidity. Our study also establishes a plausible mechanism used by *Pa*, and perhaps other gut microbes, to increase the virulence of *Vc* through induction of biofilm formation, a physiological state in which *Vc* is known to increase expression of other virulence factors critical for human infection and disease (32, 33). *Vc* biofilms have also been demonstrated to deform and even damage tissue-engineered soft epithelia mimicking the mechanics the host tissue (38), suggesting that *in vivo*-formed biofilm structures could negatively impact host gut physiology. While VPS is not usually considered a critical host colonization factor, this macromolecular structure appears to be essential for the enhancement of *Vc* host colonization induced by *Pa*. Whether this structure may mediate other *Vc*-gut microbiota species interaction remains to be studied. Many structural components, regulatory factors, and signaling transduction pathways that control biofilm formation in *Vc* have been well characterized (39), and these factors could be targeted for manipulation by other gut microbes that modulate *Vc* virulence. For example, 3,5-dimethylpyrazin-2-ol (DPO) was recently discovered as a new class of quorum-sensing autoinducer in *Vc* that binds to the transcription factor VqmA to activate expression of *vqmR*, which encodes a small regulatory RNA that downregulates *Vc* biofilm formation. The VqmA-VqmR system can be activated both *in vitro* by *Escherichia coli* and *in vivo* by *B. obeum* (5, 40), which leads to suppression of biofilm formation. Interestingly, *Pa* demonstrates the opposite tendency by promoting *Vc* biofilm formation, which indirectly supports its role in enhancing *Vc* infection, in contrast to other commensal bacteria.

Investigation into the structure-function relationship in other multispecies biofilms, such as dental biofilms, has revealed a coordinated organization of each species that allows for optimal nutrient and oxygen usage, as well as mechanical stability (41, 42). Coaggregation between *Vc* and other microbiota species has been observed (43), but these associations are not known to have a direct influence on *Vc* pathogenicity. While we did not observe any growth yield enhancement in the planktonic phase of the co-culture, there was a significant increase of *Vc* and *Pa* in the co-culture pellicle at the air-liquid interface. Thus, in addition to promoting a biofilm-associated hyper-infective state, another possible role of the dual-species biofilm in *Vc* virulence could be the optimization of nutrient sharing and distribution, or for the removal of toxic metabolites accumulated during growth. The observed temperature-dependent, plate-shaped architecture of *Pa* biofilms in the presence of *Vc* further supports the idea that the two species exist in a mutualistic partnership.

Many aspects of the *Pa*-*Vc* interaction are still unclear. Secreted small molecules produced by *Pa* do not appear to impact *Vc* as evidenced by our experiments here and prior studies where *Vc* cultured in *Pa* spent-cell supernatant did not yield result in increased biofilm formation (7). While our data suggests that hydrophobic interactions can foster the association between *Vc* and *Pa*, it is not known how this hydrophobic affinity may manifest in the context of the intestinal microbial community where *Pa* represents only a minor fraction of the total gut microbiota. Given the fact that the biofilm enhancement phenotype requires the presence of viable *Pa* cells, we hypothesize that *Pa* interacts with *Vc* to enhance biofilm formation through potential VPS-dependent and -independent mechanisms. We have shown that VPS (20) is important for *Pa*-*Vc* interactions in an animal host, but whether the VPS is directly involved in the interaction between these two species remains unknown. In addition to VPS, the extracellular matrix of the *Vc* biofilm contains several biofilm-associated proteins (i.e., Bap1, RbmA, and RbmC) and extracellular DNA (44-46), and the role of these *Vc* biofilm matrix components in promoting *Pa*-*Vc* interactions, and the nature of the plate-shaped secretion, needs further investigation. Other members of the *Paracoccus* genus are known to form biofilms and encode adhesins to facilitate surface attachment in addition to nonspecific hydrophobic interactions (47, 48), and the potential role of these adhesins in facilitating interaction with *Vc* remains to be studied.

We describe a novel interaction between *Vc* and a gut microbe initially found to bloom in patients with *Vc* infection that leads to a significant change in their biofilm behaviors, as well as an increase in the virulence of the pathogen. Our findings are also consistent with other observations that rare gut microbial species can have significant impacts on microbial ecosystems (49). This study adds to the growing number of pathogen-gut microbial species interactions that may impact outcomes in human diseases.

Materials and Methods

Prior published study sample collection and analysis

In a prior study, we enrolled household contacts of persons hospitalized with cholera at the International Centre for Diarrheal Disease Research, Bangladesh (icddr,b)(7). Briefly, in this previously published study, household contacts were followed prospectively with rectal swab sampling, 30 days of clinical symptom report, and vibriocidal titer measurements, and 16S rRNA sequencing was performed on rectal swab sampling from the day of enrollment in the study (7). Persons with evidence of *V. cholerae* infection at the time of enrollment in the study were compared to those who did not have evidence of infection in a model to detect gut microbes that were differentially abundant during *V. cholerae* infection (7). *V. cholerae* infection was defined as *V. cholerae* DNA identified on 16S rRNA sequencing or a positive *Vc* stool culture. In this previously published study, we used a machine learning method called a support vector machine (SVM), which utilizes patterns of OTU relative abundance to detect OTUs associated with infected compared to uninfected persons. This SVM was used with a recursive feature elimination algorithm that simplifies models and increases accuracy of the identification of differentially associated OTUs by removing uninformative bacterial taxa (7). For the present study, we re-examined the microbiome data from household contacts at the time of enrollment to quantify the abundance of 16s rRNA reads that mapped to *Pa* OTUs between uninfected study participants and infected participants.

Strains and culture conditions

All *V. cholerae* strains used in this study are streptomycin-resistant derivatives of C6706, a 1991 El Tor O1 clinical isolate from Peru (50). The in-frame *vpsL* deletion mutants (*vpsL*$^{-}$) used in various assays were previously described (51). *V. cholerae* strains used for microscopy experiments, Δ*vc1807*:: P_{tac} – *mNeonGreen* and *vpsL*$^{-}$ Δ*vc1807*:: P_{tac} – *mNeonGreen,* were constructed as previous described (26). The *P. aminovorans* used in our experiments is a Strep^{R} isolate derived from the ATCC type strain (ATCC #49632). *V. cholerae* and *P. aminovorans* overnight cultures were grown with aeration in LB at 30°C. Heat-killed strains were incubated at 60°C for 2 hours prior

to experimentation. Unless specified, media was supplemented with streptomycin (Sm, 100 µg/ml) and chloramphenicol (Cm, 10 µg/ml) when appropriate.

Animal studies

For establishing colonization of the microbiota species, 3-day old suckling CD-1 mice (Charles River Laboratories) were fasted for 1 hour, then orally dosed with *P. aminovorans* at a concentration of 10^7 CFU using 30-gauge plastic tubing, after which the animals were placed with a lactating dam for 10-12 hrs and monitored in accordance with the regulations of Tufts Comparative Medicine Services. This inoculation scheme was followed an additional 3 times, for a total of 4 inoculations of *P. aminovorans* over the course of 48hrs. After 48hrs, mice were infected with 10^6 CFU of *V. cholerae*, WT C6706 or mutant strain, or LB as a vehicle control in a gavage volume of 50 µl to evaluate the effect of *P. aminovorans* pre-colonization on *V. cholerae* host colonization. At 18-24hrs post-infection, animals were sacrificed, and small intestine tissue samples were collected and homogenized for CFU enumeration. WT *V. cholerae* is *lac*$^+$ and appears blue on medium containing X-gal while *P. aminovorans* appears white on the same medium.

Ethics Statement

All animal experiments were performed at and in accordance with the rules of the Tufts Comparative Medicine Services (CMS), following the guidelines of the American Veterinary Medical Association (AVMA) as well as the Guide for the Care and Use of Laboratory Animals of the National Institutes of Health. All procedures were performed with approval of the Tufts University CMS (Protocol# B 2018-99). Euthanasia was performed in accordance with guidelines provided by the AVMA and was approved by the Tufts CMS. The previously published study from which Fig. 1 is derived (7) received approval from the Ethical Review Committee at the icddr,b and the institutional review boards of Massachusetts General Hospital and the Duke University Health System. Participants or their guardians provided written informed consent.

Pellicle composition analysis

To assess pellicle composition, overnight cultures of *V. cholerae* and *P. aminovorans* were inoculated into glass culture tubes (18 x 150 mm) containing 2mL LB media in a ratio of 1:10 *V. cholerae* (10^6) to *P. aminovorans* (10^7) CFU, and co-cultures were allowed to grow statically at room temperature for 3 days. Following static growth, floating pellicles were carefully transferred into sterile 1.5mL Eppendorf tubes containing 1mL LB, and samples were gently spun down to wash away any planktonic bacteria. Planktonic cells were removed, and cell pellets of pellicle samples were resuspended in 1mL of fresh LB media. All samples including supernatant from the pellicle wash step, were serial diluted and plated on Sm/X-Gal media to differentiate *V. cholerae* (blue) and *P. aminovorans* (white) colonies.

Crystal violet biomass assays

Crystal violet biofilm assays were performed as described previously in 96-well flat bottom clear, tissue-culture treated polystyrene microplates (ThermoFisher) (19). Untreated hydrophobic polystyrene microplates (Greiner Bio-One) were also used. In each well, *V. cholerae* (10^6 CFUs) and/or *P. aminovorans* (10^6 or 10^7 CFUs) were inoculated into 200µL of medium. For experiments involving spent culture supernatants, *V. cholerae* (10^6 CFUs) were inoculated into each well containing 200 µL of reconditioned supernatants (80% (v/v) filtered spent culture medium and 20% (v/v) 5× LB). Plates were then sealed using a gas permeable sealing film (BrandTech) and incubated at 37°C. Planktonic culture was removed after 24 hours of incubation, plates were washed with distilled water once. Attached biofilms were stained with 0.1% crystal violet at room temperature for 15-20 min. The amount of biomass adhered to the sides of each well was quantified by dissolving the crystal violet in 95% ethanol and the absorbance of the resulting solution was measured at 550 nm or 570 nm using a plate reader.

Microbial Adhesion to Hydrocarbon (MATH) assay

Overnight cultures *P. aminovorans* were grown at 30°C with agitation. MATH was conducted as previous described (52, 53). Briefly, samples were washed twice by centrifuging at 4,500 × g for 10 minutes at room temperature, removing supernatant, and re-suspending in fresh LB broth. Samples were then normalized to an OD_{600} of ~0.5 and 4 ml were aliquoted into borosilicate glass test tubes (Pyrex). Test samples were treated with 1 ml, 0.5 ml, and 0.1 ml of xylene (Fisher Chemical). Samples without xylene were used as control. After 45 seconds of vortexing at the max setting, samples were incubated on the lab bench for 30 minutes. The OD_{600} of the aqueous layer (beneath the xylene bubbles) was measured. Percent adherence is calculated as [1 - (OD test samples) / (OD control)] × 100.

Microscopy

Liquid LB culture of *V. cholerae*, *P. aminovorans*, and co-cultures (*Pa*:*Vc* = 10:1) were prepared according to procedures described above. For growth of submerged biofilms, 100 µL of each diluted culture was added to a well in a glass-bottomed 96 well plate (MatTek) and grown at 37°C for 24 hours or at room temperature for 48 hours. For the room temperature culture, the culture media was replaced with 100 µL of fresh LB after 24 hours. At the end of the biofilm growth, the surface attached biofilms were carefully washed with 100 µL LB media twice and subsequently stained with 4 µg/mL FM 4-64 (ThermoFisher). The stained biofilms are imaged with a Nikon-W1 confocal microscope using 60× water objective (numerical aperture = 1.2). Typically, an area of 663 × 663 μm^2 is captured for large-scale quantification with a *z*-step size of 3 µm and a pixel size of 216 nm. For zoom-in view, the *z*-step size is 1 µm and the pixel size is 108 nm. The mNeonGreen expressed by *Vc* is imaged at 488 nm excitation and FM 4-64 at 561 nm with the corresponding filters. All presented images are raw images processed from Nikon Element software. The biofilm mass quantification is performed with built-in thresholding functions in Nikon Element software.

Statistics

Error bars in the figures depict either standard deviations of the means or the median with a 95% confidence interval as indicted. Based on the experimental design, either standard *t*-test or Mann-Whitney test were used to compare treatment groups as indicated in each figure legend.

Acknowledgments

We thank members in the Ng and Weil Labs for helpful discussions. We acknowledge Ed Ryan for his assistance in reviewing the manuscript. A.A.W and W-L.N. received support from a Rozan Award from Tufts University School of Medicine for this project. A.A.W. support was provided by AI123494 from the National Institute of Allergy and Infectious Diseases (NIAID). W-L.N was supported by AI121337. J.Y. holds a Career Award at the Scientific Interface from the Burroughs Wellcome Fund.

References

1. A. Camacho *et al.*, Cholera epidemic in Yemen, 2016-18: an analysis of surveillance data. *Lancet Glob Health* **6**, e680-e690 (2018).
2. F. J. Luquero *et al.*, Mortality Rates during Cholera Epidemic, Haiti, 2010-2011. *Emerg Infect Dis* **22**, 410-416 (2016).
3. A. A. Weil, E. T. Ryan, Cholera: recent updates. *Curr Opin Infect Dis* **31**, 455-461 (2018).
4. S. Alavi *et al.*, Interpersonal Gut Microbiome Variation Drives Susceptibility and Resistance to Cholera Infection. *Cell* **181**, 1533-1546.e1513 (2020).
5. A. Hsiao *et al.*, Members of the human gut microbiota involved in recovery from *Vibrio cholerae* infection. *Nature* **515**, 423-426 (2014).

6. I. Levade *et al.*, Predicting Vibrio cholerae infection and disease severity using metagenomics in a prospective cohort study. *J Infect Dis* 10.1093/infdis/jiaa358 (2020).

7. F. S. Midani *et al.*, Human Gut Microbiota Predicts Susceptibility to *Vibrio cholerae* Infection. *J Infect Dis* 10.1093/infdis/jiy192 (2018).

8. P. T. McKenney, E. G. Pamer, From Hype to Hope: The Gut Microbiota in Enteric Infectious Disease. *Cell* **163**, 1326-1332 (2015).

9. R. Freter, The fatal enteric cholera infection in the guinea pig, achieved by inhibition of normal enteric flora. *J Infect Dis* **97**, 57-65 (1955).

10. E. Nygren, B. L. Li, J. Holmgren, S. R. Attridge, Establishment of an Adult Mouse Model for Direct Evaluation of the Efficacy of Vaccines against *Vibrio cholerae*. *Infection and Immunity* **77**, 3475 (2009).

11. W. Zhao, F. Caro, W. Robins, J. J. Mekalanos, Antagonism toward the intestinal microbiota and its effect on *Vibrio cholerae* virulence. *Science* **359**, 210-213 (2018).

12. S. A. Jung, C. A. Chapman, W. L. Ng, Quadruple quorum-sensing inputs control Vibrio cholerae virulence and maintain system robustness. *PLoS Pathog* **11**, e1004837 (2015).

13. S. Watve *et al.*, Parallel quorum-sensing system in Vibrio cholerae prevents signal interference inside the host. *PLoS Pathog* **16**, e1008313 (2020).

14. J. S. You *et al.*, Commensal-derived metabolites govern *Vibrio cholerae* pathogenesis in host intestine. *Microbiome* **7**, 132 (2019).

15. T. Yatsunenko *et al.*, Human gut microbiome viewed across age and geography. *Nature* **486**, 222-227 (2012).

16. T. Urakami, H. Araki, H. Oyanagi, K. Suzuki, K. Komagata, Paracoccus aminophilus sp. nov. and Paracoccus aminovorans sp. nov., which utilize N,N-dimethylformamide. *International journal of systematic bacteriology* **40**, 287-291 (1990).

17. L. A. David *et al.*, Gut microbial succession follows acute secretory diarrhea in humans. *mBio* **6**, e00381-00315 (2015).

18. K. E. Klose, The suckling mouse model of cholera. *Trends Microbiol* **8**, 189-191 (2000).

19. G. A. O'Toole, Microtiter dish biofilm formation assay. *J Vis Exp* 10.3791/2437 (2011).

20. F. H. Yildiz, G. K. Schoolnik, Vibrio cholerae O1 El Tor: identification of a gene cluster required for the rugose colony type, exopolysaccharide production, chlorine resistance, and biofilm formation. *Proc Natl Acad Sci U S A* **96**, 4028-4033 (1999).

21. Y. A. Millet *et al.*, Insights into Vibrio cholerae intestinal colonization from monitoring fluorescently labeled bacteria. *PLoS Pathog* **10**, e1004405 (2014).

22. C. D. Nadell, K. Drescher, N. S. Wingreen, B. L. Bassler, Extracellular matrix structure governs invasion resistance in bacterial biofilms. *ISME J* **9**, 1700-1709 (2015).

23. R. Hartmann *et al.*, Emergence of three-dimensional order and structure in growing biofilms. *Nat Phys* **15**, 251-256 (2019).

24. J. Yan, A. G. Sharo, H. A. Stone, N. S. Wingreen, B. L. Bassler, Vibrio cholerae biofilm growth program and architecture revealed by single-cell live imaging. *Proc Natl Acad Sci U S A* **113**, E5337-5343 (2016).

25. N. C. Shaner *et al.*, A bright monomeric green fluorescent protein derived from Branchiostoma lanceolatum. *Nat Methods* **10**, 407-409 (2013).

26. A. B. Dalia, E. McDonough, A. Camilli, Multiplex genome editing by natural transformation. *Proc Natl Acad Sci U S A* **111**, 8937-8942 (2014).

27. L. Townsley, M. P. Sison Mangus, S. Mehic, F. H. Yildiz, Response of Vibrio cholerae to Low-Temperature Shifts: CspV Regulation of Type VI Secretion, Biofilm Formation, and Association with Zooplankton. *Appl Environ Microbiol* **82**, 4441-4452 (2016).

28. E. C. Hollenbeck *et al.*, Molecular determinants of mechanical properties of V. cholerae biofilms at the air-liquid interface. *Biophys J* **107**, 2245-2252 (2014).

29. J. Yan *et al.*, Bacterial Biofilm Material Properties Enable Removal and Transfer by Capillary Peeling. *Adv Mater* **30**, e1804153 (2018).

30. V. Carniello, B. W. Peterson, H. C. van der Mei, H. J. Busscher, Physico-chemistry from initial bacterial adhesion to surface-programmed biofilm growth. *Adv Colloid Interface Sci* **261**, 1-14 (2018).

31. H. C. van der Mei, J. de Vries, H. J. Busscher, Hydrophobic and electrostatic cell surface properties of thermophilic dairy streptococci. *Appl Environ Microbiol* **59**, 4305-4312 (1993).

32. R. Tamayo, B. Patimalla, A. Camilli, Growth in a biofilm induces a hyperinfectious phenotype in *Vibrio cholerae*. *Infect Immun* **78**, 3560-3569 (2010).

33. A. L. Gallego-Hernandez *et al.*, Upregulation of virulence genes promotes *Vibrio cholerae* biofilm hyperinfectivity. *Proc Natl Acad Sci U S A* **117**, 11010-11017 (2020).

34. J. Zhu, J. J. Mekalanos, Quorum sensing-dependent biofilms enhance colonization in *Vibrio cholerae*. *Dev Cell* **5**, 647-656 (2003).

35. J. C. N. Fong, K. A. Syed, K. E. Klose, F. H. Yildiz, Role of Vibrio polysaccharide (vps) genes in VPS production, biofilm formation and Vibrio cholerae pathogenesis. *Microbiology (Reading)* **156**, 2757-2769 (2010).

36. C. Ubeda, A. Djukovic, S. Isaac, Roles of the intestinal microbiota in pathogen protection. *Clinical & Translational Immunology* **6**, e128 (2017).

37. A. A. Weil, R. L. Becker, J. B. Harris, *Vibrio cholerae* at the Intersection of Immunity and the Microbiome. *mSphere* **4**, e00597-00519 (2019).

38. A. Cont, T. Rossy, Z. Al-Mayyah, A. Persat, Biofilms deform soft surfaces and disrupt epithelia. *Elife* **9**, e56533 (2020).

39. J. K. Teschler *et al.*, Living in the matrix: assembly and control of Vibrio cholerae biofilms. *Nat Rev Microbiol* **13**, 255-268 (2015).

40. K. Papenfort *et al.*, A Vibrio cholerae autoinducer-receptor pair that controls biofilm formation. *Nat Chem Biol* **13**, 551-557 (2017).

41. B. B. Christensen, J. A. Haagensen, A. Heydorn, S. Molin, Metabolic commensalism and competition in a two-species microbial consortium. *Appl Environ Microbiol* **68**, 2495-2502 (2002).

42. J. L. Mark Welch, B. J. Rossetti, C. W. Rieken, F. E. Dewhirst, G. G. Borisy, Biogeography of a human oral microbiome at the micron scale. *Proc Natl Acad Sci U S A* **113**, E791-800 (2016).

43. Y. S. Toh *et al.*, Role of coaggregation in the pathogenicity and prolonged colonisation of *Vibrio cholerae*. *Med Microbiol Immunol* **208**, 793-809 (2019).

44. C. Absalon, K. Van Dellen, P. I. Watnick, A communal bacterial adhesin anchors biofilm and bystander cells to surfaces. *PLoS Pathog* **7**, e1002210 (2011).

45. V. Berk *et al.*, Molecular architecture and assembly principles of Vibrio cholerae biofilms. *Science* **337**, 236-239 (2012).

46. J. C. Fong, K. Karplus, G. K. Schoolnik, F. H. Yildiz, Identification and characterization of RbmA, a novel protein required for the development of rugose colony morphology and biofilm structure in Vibrio cholerae. *J Bacteriol* **188**, 1049-1059 (2006).

47. K. Yoshida, M. Toyofuku, N. Obana, N. Nomura, Biofilm formation by Paracoccus denitrificans requires a type I secretion system-dependent adhesin BapA. *FEMS Microbiol Lett* **364** (2017).

48. C. S. Srinandan, V. Jadav, D. Cecilia, A. S. Nerurkar, Nutrients determine the spatial architecture of Paracoccus sp. biofilm. *Biofouling* **26**, 449-459 (2010).

49. A. Jousset *et al.*, Where less may be more: how the rare biosphere pulls ecosystems strings. *ISME J* **11**, 853-862 (2017).

50. K. H. Thelin, R. K. Taylor, Toxin-coregulated pilus, but not mannose-sensitive hemagglutinin, is required for colonization by Vibrio cholerae O1 El Tor biotype and O139 strains. *Infect Immun* **64**, 2853-2856 (1996).

51. C. M. Waters, W. Lu, J. D. Rabinowitz, B. L. Bassler, Quorum sensing controls biofilm formation in Vibrio cholerae through modulation of cyclic di-GMP levels and repression of vpsT. *J Bacteriol* **190**, 2527-2536 (2008).

52. O. Niderman-Meyer, T. Zeidman, E. Shimoni, Y. Kashi, Mechanisms involved in governing adherence of Vibrio cholerae to granular starch. *Applied and environmental microbiology* **76**, 1034-1043 (2010).

53. M. Rosenberg, Bacterial adherence to hydrocarbons: a useful technique for studying cell surface hydrophobicity. *FEMS Microbiology Letters* **22**, 289-295 (1984).

Figures and Tables

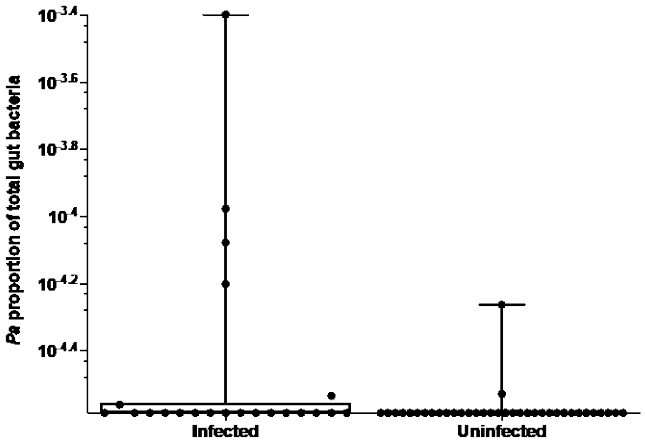

Figure 1. *Pa* is more abundant in persons with *Vc* infection compared to uninfected persons. In a prior study of household contacts of cholera patients in Bangladesh (7), we measured *Pa* abundance using 16S rRNA in rectal swabs collected from individuals with *Vc* infection (*n* = 22) compared to uninfected individuals (n=36). In this study, total sum normalization was applied to OTU counts from each sample, and a median of 37,958 mapped reads per sample were generated(7). Based on sequencing data only, the estimated limit of detection for a *Pa* OTU is 2.0×10^{-5}. All data points are shown, and boxes indicate interquartile range. Bars mark the maximum and minimum values. The collected data were compared with non-parametric unpaired Mann-Whitney U testing, *P* = 0.009.

.

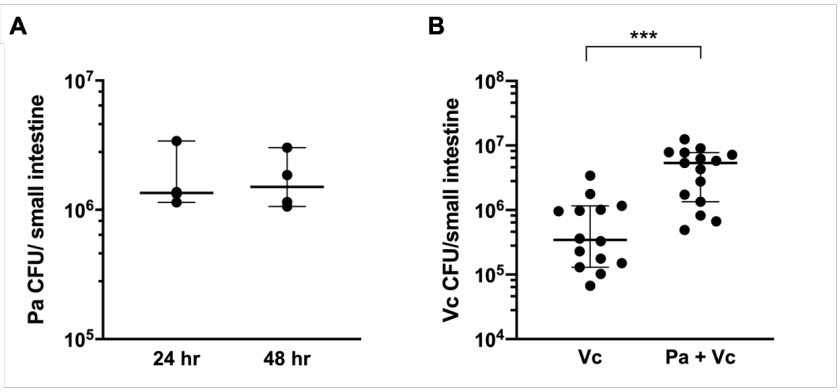

Figure 2. Establishment of *Pa* colonization in the infant mouse intestine. (A) 3 day-old infant mice were intragastrically inoculated with 10^7 CFU of *Pa* every 12 hours for a period of 24 hr (2 doses) or 48 hr (4 doses). At each time point mice were sacrificed and CFU were enumerated by plating serial dilutions of small intestine samples on selective media. **(B)** 3 day-old infant mice were intragastrically inoculated with LB or 10^7 CFU of *Pa* every 12 hours for a period of 48 hr, and subsequently infected with 10^6 CFU of WT *Vc.* Mice were sacrificed 20-24 hr post-infection and the small intestine samples were taken to enumerate *Vc*. Bars on graphs depict median value with 95% confidence interval (CI) and individual data points plotted. Unpaired non-parametric *t*-test (Mann-Whitney); *** $P \leq 0.001$.

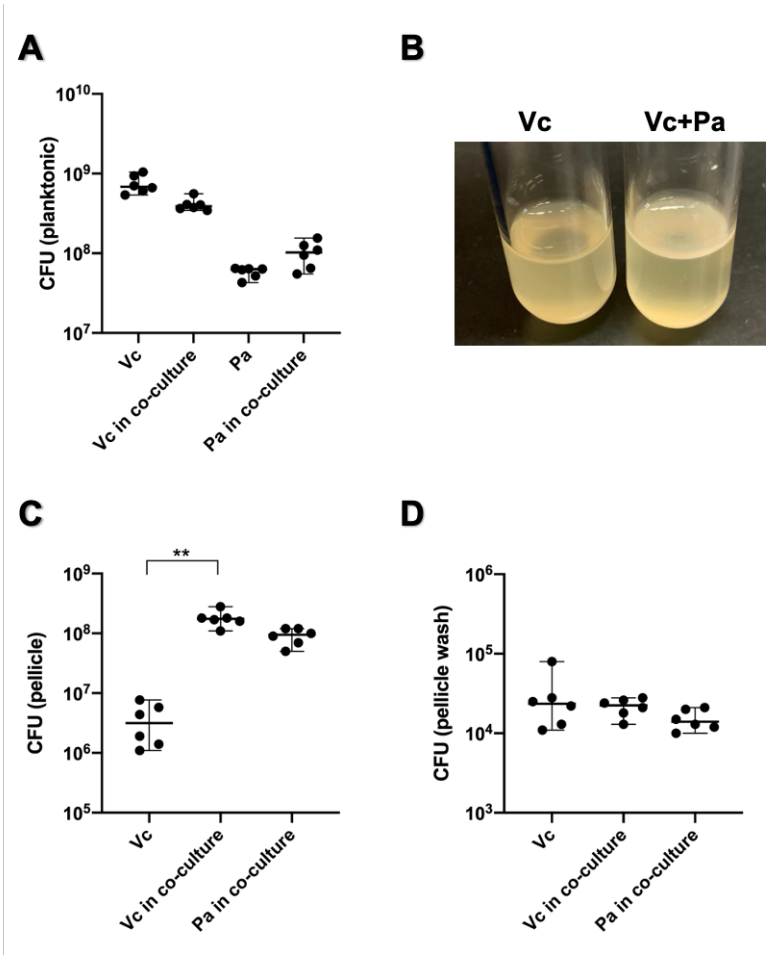

Figure 3. *Pa* promotes biofilm formation of *Vc*. (A) Planktonic cell counts from cultures used for pellicle analysis of *Vc* and *Pa* grown together or in monoculture at room temperature for 72 hrs. **(B)** Representative images of pellicles formed by *Vc* grown in monoculture and in co-culture with *Pa*. CFU counts of each strain in **(C)** pellicle samples and **(D)** spent medium used to wash the pellicle. Bars on graphs depict median value with 95% confidence interval (CI) and individual data points plotted. Unpaired non-parametric *t*-test (Mann-Whitney): ** $P \leq 0.01$.

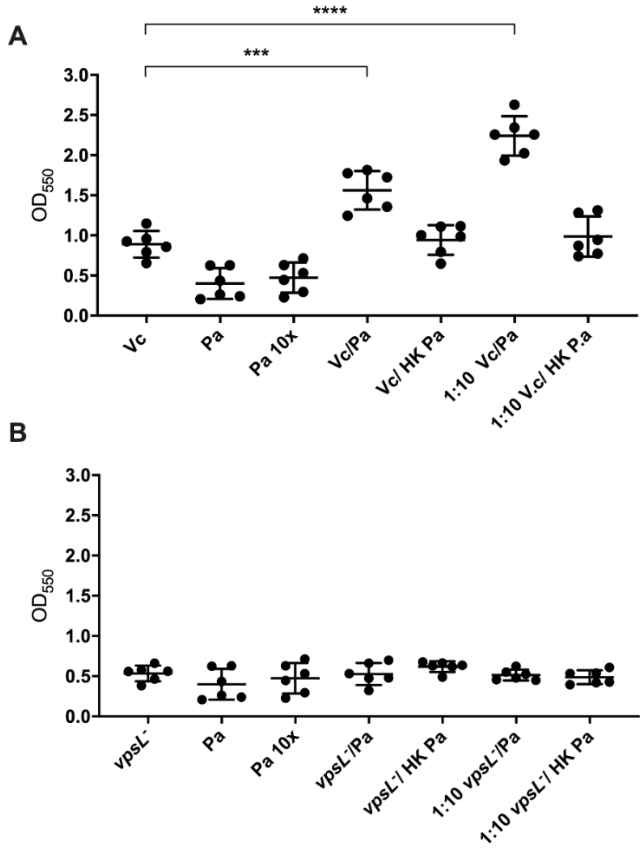

Figure 4. *Pa* increases biofilm production in *Vc*. Crystal violet assays were performed in 96-well microtiter plates to quantify biofilm formation. Overnight-grown **(A)** wild-type *Vc* or **(B)** *vpsL*$^{-}$ mutant and *Pa* cultures were diluted to a final concentration of 10^6 CFU in a total volume of 200 µL/well. In samples containing a 1:10 ratio of *Vc*/*Pa*, *Pa* was diluted to a final concentration of 10^7 CFU. Samples with heat-killed (HK) *Pa* are specified in the X-axis. Microtiter plates were incubated at 37 °C for 24 hr. Crystal violet staining and ethanol solubilization were performed as previously described (19). Absorbance of the crystal violet stain was measured at 550 nm using a Biotek Synergy HTX plate reader. Data is represented with horizontal lines indicating the mean with standard deviation. Unpaired *t*-test; ***$P \leq 0.001$, ****$P \leq 0.0001$.

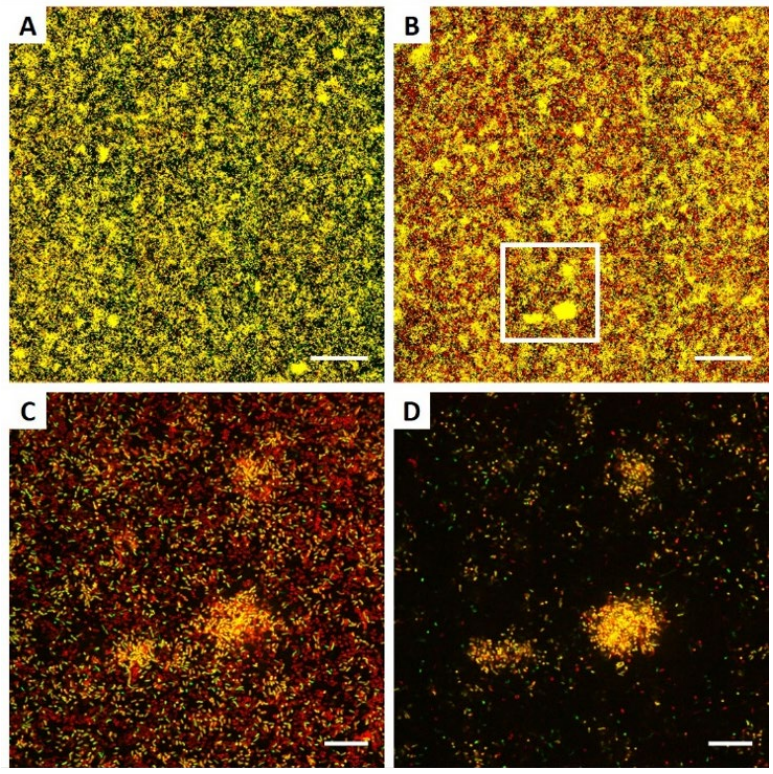

Figure 5. (A,B) Maximum intensity projection of large views of **(A)** *Vc* biofilms and **(B)** *Vc* and *Pa* dual-species biofilm. **(C,D)** Zoom-in view of the region highlighted in B (white square) at the glass surface **(C)** and 6 µm above the surface **(D**). All cells are stained with FM 4-64 and *Vc* cells constitutively express mNeonGreen (*Vc*: yellow; *Pa*:Red). Scale bars are 100 µm in A,B and 20 µm in C,D.

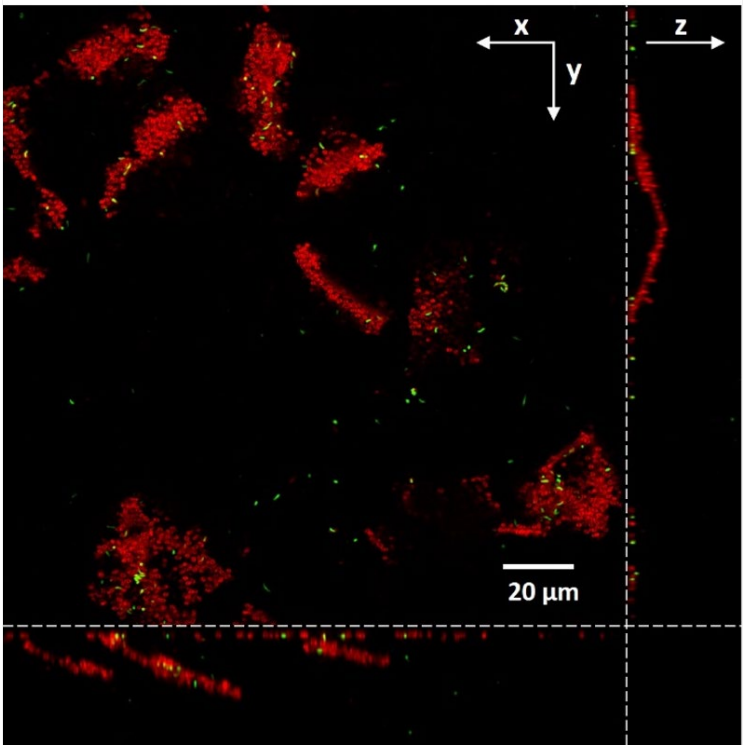

Figure 6. *Pa* forms a plate-shaped three-dimensional architecture when grown at 37°C in the presence of *Vc.* Cross-sectional views of biofilm structure formed by co-culturing *Vc* and *Pa* at 37°C for 24 hours. All cells are stained with FM 4-64. *Vc* cells constitutively express mNeonGreen (*Pa*: Red; *Vc*:Green).

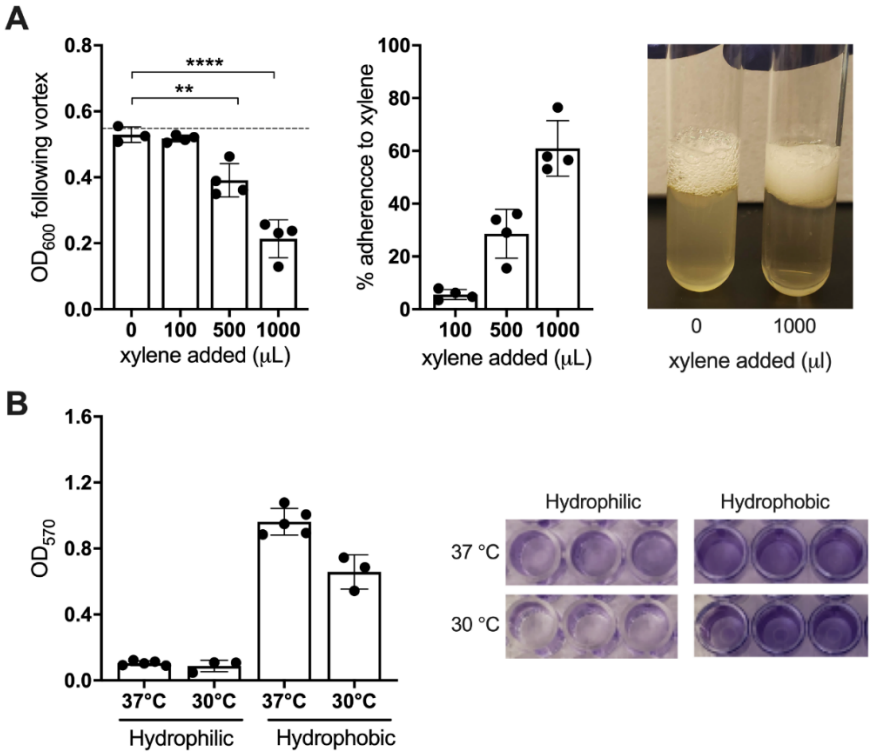

Figure 7. Hydrophobicity of *Pa* contributes to dual-species biofilm. (A) OD_{600} of aqueous layer, percent adherence to hydrocarbon, and representative photo of microbial adhesion to hydrocarbon (MATH) assay using 1 mL xylene and 4 mL of *Pa* in LB media. Gray dotted line indicates starting OD600 **(B)** Crystal violet assays of *Pa* in hydrophilic (TC-treated) or hydrophobic (untreated) polystyrene microtiter plates. 10^7 CFU per well *Pa* were incubated at 37 °C and 30°C for 24 hrs. Crystal violet staining and ethanol solubilization was performed and absorbance of the CV stain was measured at 570 nm. Data is represented with horizontal lines indicated mean with SD. Unpaired one-way ANOVA; $^{**}P \leq 0.01$, $^{****}P \leq 0.0001$.

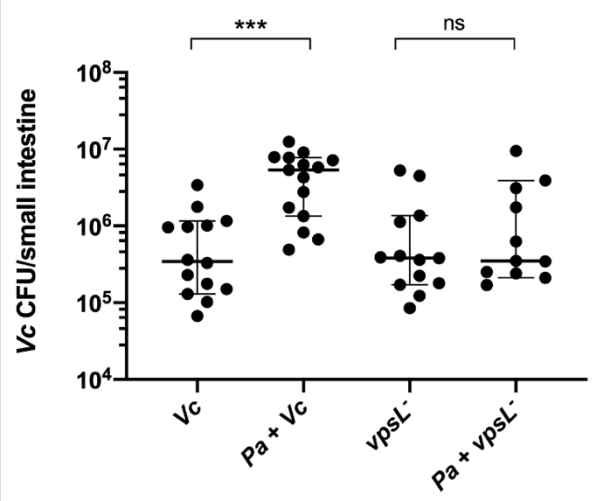

Figure 8. The enhanced colonization phenotype in the presence of *Pa* is dependent the ability of *Vc* to produce VPS. 3 day-old infant mice were intragastrically inoculated with LB or 10^7 CFU of *Pa* every 12 hours for a period of 48 hours, and subsequently infected with 10^6 CFU of a *Vc* strain defective for extracellular matrix production (*vpsL*$^-$). Mice were sacrificed 20-24 hr post-infection and small intestine samples were taken to enumerate *Vc* CFU. Data from infection with the wild-type C6706 strain (Fig. 2B) is shown again here for comparison purposes. Each symbol represents an individual mouse and data is represented with horizontal lines indicating the median with a 95% confidence interval. Unpaired non-parametric *t*-test (Mann-Whitney); ns $P > 0.05$, *** $P \leq 0.001$.

Supplementary Information for

Impact of a human gut microbe on *Vibrio cholerae* host colonization through biofilm enhancement

Kelsey Barrasso[1,2], Denise Chac[3], Meti D. Debela[4], Jason B. Harris[4,5], Regina C. LaRocque[4], Firas S. Midani[6], Firdausi Qadri[7], Jing Yan[8], Ana A. Weil[3,*], Wai-Leung Ng[1,2,*]

Corresponding authors: Ana A. Weil and Wai-Leung Ng
Email: anaweil@uw.edu wai-leung.ng@tufts.edu

This PDF file includes:

Figures S1 to S5 (not allowed for Brief Reports)
SI References

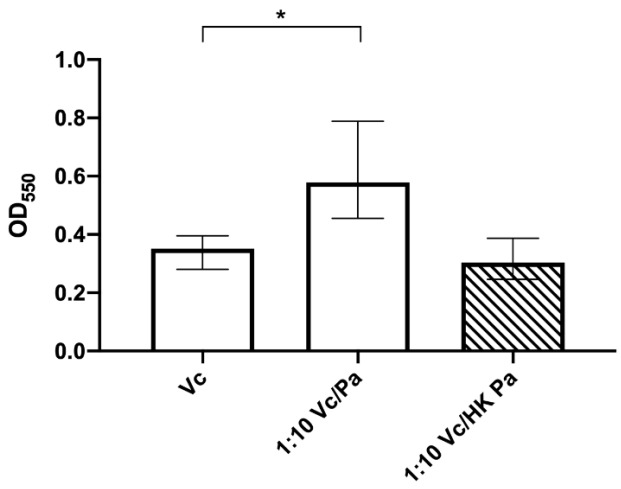

Fig. S1. Established *Pa* cultures increase biofilm production in *Vc*. Biofilm formation assays were performed in 96-well microtiter plates. *Pa* was diluted in LB to a concentration of 10^7 CFU and grown for 24hr before the addition of WT *Vc*. WT *Vc* was then diluted in LB to a concentration of 10^6 CFU and added to wells. Plates were incubated for an additional 24hr before crystal violet staining to quantify biofilm biomass. Crystal violet staining and ethanol solubilization were performed as previously described (1). Absorbance of the crystal violet stain was measured at 550 nm using a Biotek Synergy HTX plate reader. Samples with heat-killed (HK) *Pa* are delineated by hatched bars. Data is represented with horizontal lines indicating the median with 95% confidence interval. Unpaired non-parametric t-test (Mann-Whitney); * $P \leq 0.05$.

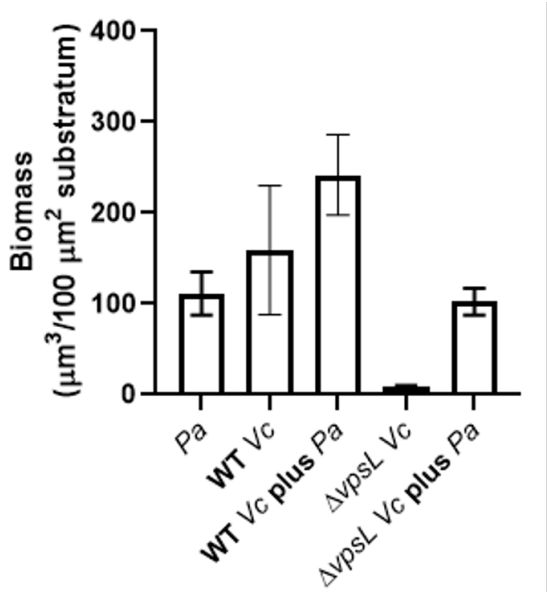

Fig. S2. Quantification of biofilm mass by microscopy. Quantification is based on FM 4-64 stain for biofilms grown at room temperature for 48 hours. Data is from 3 biological replicates; error bars correspond to standard derivations.

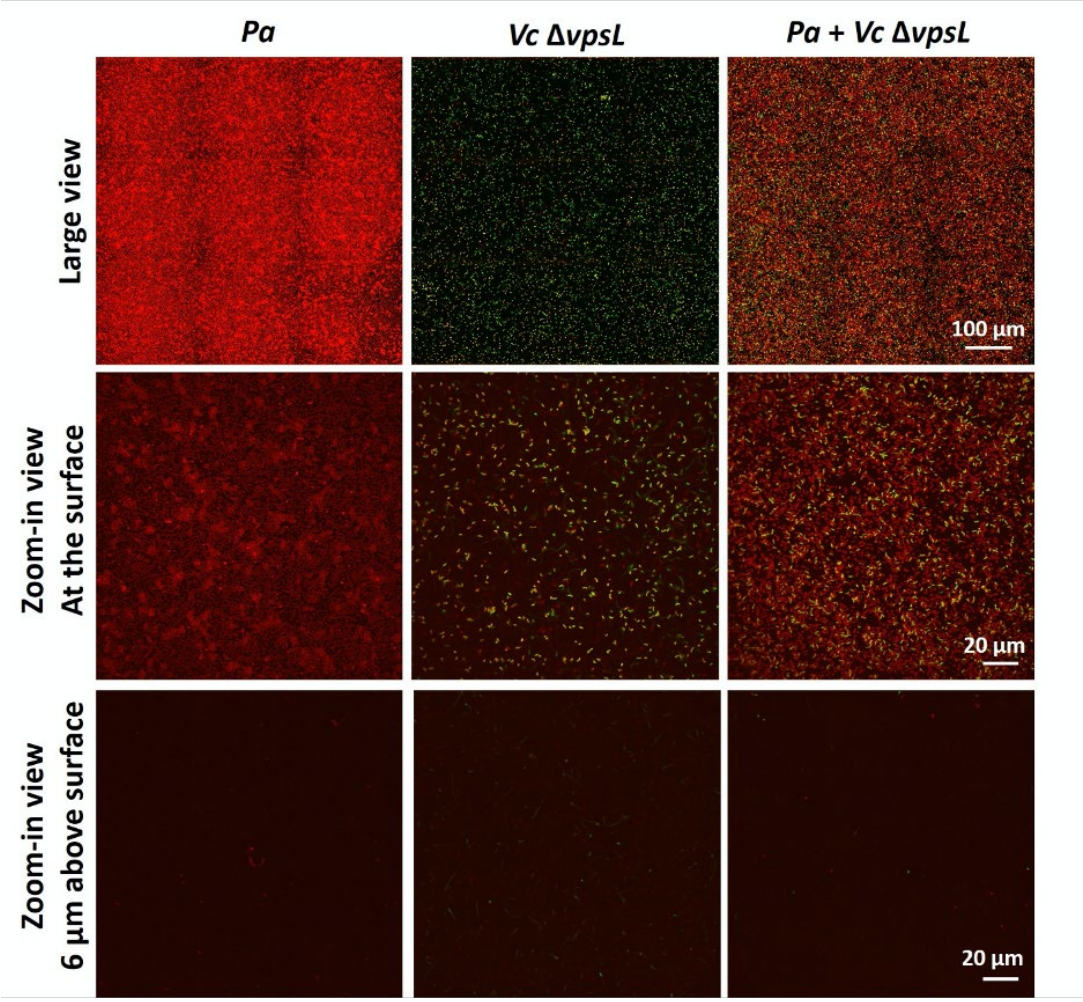

Fig. S3. *Pa* and a *vpsL*⁻ *V. cholerae* mutant do not form three-dimensional biofilm structures, alone or in co-culture. Biofilm structures formed by *Pa* alone (left column), *Vc vpsL*⁻ mutant (middle column), and a coculture of *Pa* and *Vc vpsL*⁻ mutant (right column). *Pa* cells form a monolayer on surface with local dense domains. Neither *Pa* nor *Vc vpsL*⁻ mutant forms any 3D biofilm. The structure in the coculture can be considered as an addition of *Pa* biofilms and *Vc vpsL*⁻ cells.

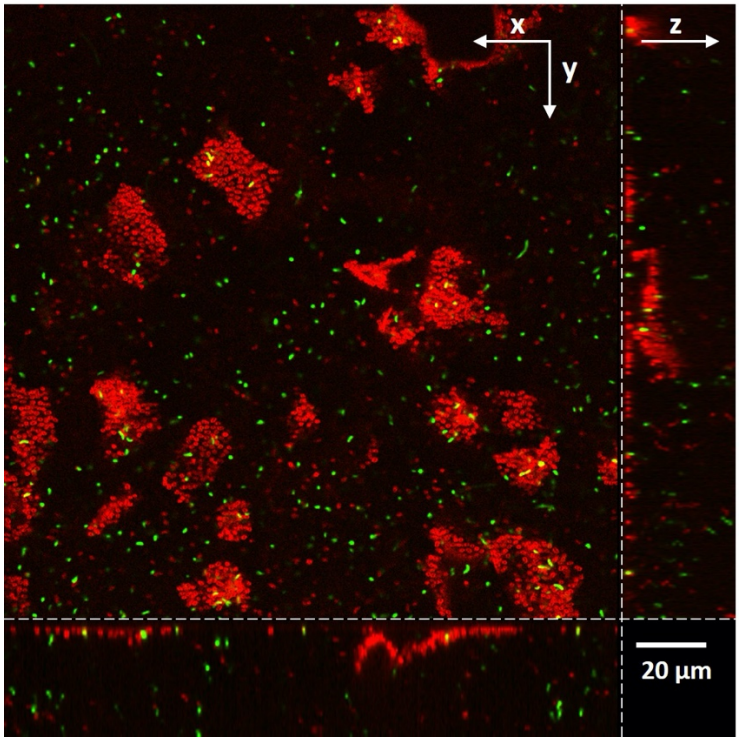

Fig. S4. The plate-shaped secretion at 37°C in *Vc* culture is independent of VPS. Cross-sectional views of biofilm structure formed by co-culturing *vpsL*⁻ *Vc* and *Pa* at 37°C for 24 hour. Cells are stained with FM 4-64. *vpsL*⁻ *Vc* cells constitutively express mNeonGreen (*Pa*:red; *Vc*:Green).

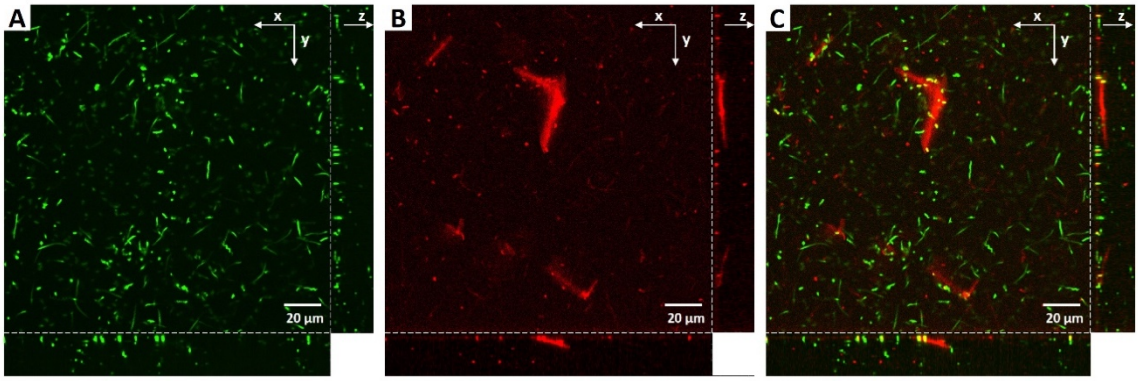

Fig. S5. Staining of the plate-shaped secretion. Cross-sectional views of the secretion structure formed by WT *Vc* monoculture grown at 37°C for 24 hour, excited at (A) 488 nm; (B) 561 nm. C shows an overlay of the two channels. The *Vc* cells constitutively express mNeonGreen. The staining solution contains 4 µg/mL FM 4-64. The plate shaped secretion shows weak signal that is consistently stronger than the background.

SI References

1. G. A. O'Toole, Microtiter dish biofilm formation assay. *J Vis Exp* 10.3791/2437 (2011).